

Neutrinos from SN 1987A

1. Determining the Neutrino Temperature and Total Emitted Energy

In this chapter, we will analyze the neutrino events from SN 1987A to see what can, and cannot, be inferred from them. We follow the discussion in a recent paper by Lattimer and Yahil.¹ The published data²⁻³ consist of detection times (t), estimated positron energies (E_e) and positron angles (θ) with respect to the Large Magellanic Cloud.

#	Kamioka				IMB			
	t (s)	E_e (MeV)	θ	$E_{\bar{\nu}_e}$ (MeV)	t (s)	E_e (MeV)	θ	$E_{\bar{\nu}_e}$ (MeV)
1	0.0	20.0 ± 2.9	18 ± 18	21.3 ± 2.9	0.0	38 ± 9.5	74 ± 15	40.5 ± 10.1
2	0.107	13.5 ± 3.2	15 ± 27	14.8 ± 3.2	0.42	37 ± 9.3	52 ± 15	38.9 ± 9.6
3	0.303	7.5 ± 2.0	108 ± 32	8.9 ± 2.05	0.65	40 ± 10	56 ± 15	42.1 ± 10.4
4	0.324	9.2 ± 2.7	70 ± 30	10.6 ± 2.75	1.15	35 ± 8.8	63 ± 15	37.0 ± 9.2
5	0.507	12.8 ± 2.9	135 ± 23	14.4 ± 3.05	1.57	29 ± 7.3	40 ± 15	30.5 ± 7.4
6	1.541	35.4 ± 8.0	32 ± 16	36.9 ± 8.1	2.69	37 ± 9.3	52 ± 15	38.9 ± 9.6
7	1.728	21.0 ± 4.2	30 ± 18	22.4 ± 4.25	5.01	20 ± 5	39 ± 15	21.4 ± 5.1
8	1.915	19.8 ± 3.2	38 ± 22	21.2 ± 3.25	5.59	24 ± 6	102 ± 15	26.1 ± 6.4
9	9.219	8.6 ± 2.7	122 ± 30	10.0 ± 2.8				
10	10.433	13.0 ± 2.6	49 ± 26	14.4 ± 2.65				
11	12.439	8.9 ± 1.9	91 ± 39	10.3 ± 1.95				

Table 1.1: Observed Events and Inferred Neutrino Energies

These data are collected in Table 1.1. It is not possible, except in a statistical sense, to determine which events are due to ν scattering and which to $\bar{\nu}_e$ absorption on protons. The distribution of angles suggests that all but at most one or two of the detections were absorptions. Since theoretical expectations are that less than 5% of the events were due to scattering, we assume here that none were, and the neutrino energies listed

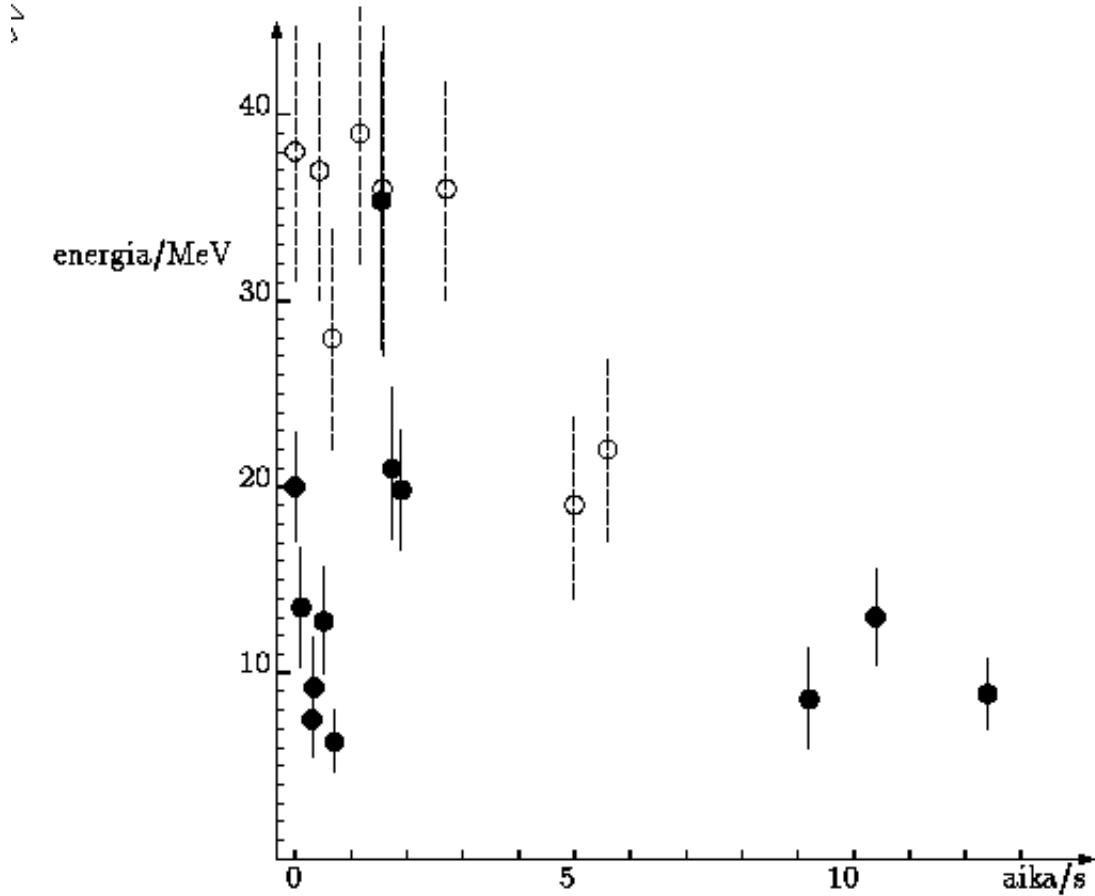


Figure 1.1:

in the table were calculated from the electron properties via

$$E_{\bar{\nu}} = \frac{E_e + \Delta + (\Delta^2 - m_e^2) / 2m_p}{1 - (E_e - p_e \cos(\theta)) / m_p}, \quad (1.1)$$

where $\Delta = (m_n - m_p)c^2$ and p_e is the positron momentum. Our conclusions are not sensitive to the assumption of how many of the events were scatterings. The inferred neutrino energy is also well approximated by the detected energy plus 1.3 MeV, the neutron-proton mass difference, regardless of the observed angle.

For our assumed spectrum, the differential distribution function of the antineutrinos incident on the detector is proportional to $E_{\bar{\nu}}^2 f(E_{\bar{\nu}}/T)$, where $f(E_{\bar{\nu}}/T)$ is the Fermi distribution, and T is the effective temperature. For simplicity, we now call the antineutrino energy $E_{\bar{\nu}}$. Because the energies and temperature we are interested in are those observed at the Earth, there is no need to include source redshift corrections. However, redshift corrections must be and were indeed included in the models discussed in the previous

section. The average neutrino energy at the source is then

$$\langle E_\nu \rangle_s = \frac{\int_0^\infty E_\nu^3 f(E_\nu/T) dE_\nu}{\int_0^\infty E_\nu^2 f(E_\nu/T) dE_\nu} = \frac{F_3(0)}{F_2(0)} T \simeq 3.15T, \quad (1.2)$$

where the F_i are the standard Fermi integrals.

In order to predict the energy distribution of the detected neutrino events, the distribution at the source must be multiplied by the neutrino absorption opacity, $\kappa(E_\nu) = \kappa_o E_e p_e$, the detector mass, M , and its detection efficiency $W(E_\nu)$. Here, $\kappa_o = 9 \times 10^{-44}$ cm² per proton (see §7.2). The existence of a detector threshold, H , the energy below which events are rejected as noise, must also be included. In practice, $W(H) \leq 0.5$.

	Fiducial Mass M (kt)	Threshold H	Efficiency $W(E_\nu)$	Error $\Delta(E_\nu)$
Kamioka	2.14	7	$1 - 4.9e^{-E_\nu/3.6}$	$0.20 + 0.19E_\nu$
IMB	5.0	20	$1 - 3e^{-E_\nu/16}$	$-0.38 + 0.26E_\nu$

Table 1.2: Detector Characteristics (all energies in MeV), as of Feb. 1987.

We take the detector masses, thresholds and efficiencies from the discovery papers, and these are listed in Table 1.2. Since we have estimated in Chapter 8 that the average emitted $\bar{\nu}_e$ energy is of order 10 MeV, we expect that IMB will only sample the high energy tail of the spectrum. It is interesting that since the characteristics of these detectors are so different, a determination of the temperature can easily be made on this basis (see below).

Additional account should be taken of the experimental errors in the determination of the neutrino energy. Let the detector response function $R(E_\nu, x)$ be the differential conditional probability for measuring an observed neutrino energy E_ν , given a true neutrino energy x . (Unless otherwise stated, we henceforth maintain the distinction between the two energies by using E_ν and x to refer only to the observed and true neutrino energies, respectively.) The distribution of observed energies is therefore an integral over all possible true neutrino energies,

$$N(E_\nu) \propto \int_H^\infty x^2 f(x/T) \kappa(x) W(x) R(E_\nu, x) dx. \quad (1.3)$$

Kolb, Stebbins and Turner⁴ have pointed out that, since the combination of opacity, efficiency and incoming spectrum is a steep function of the energy, the error in the determination of the detected neutrino energy is not evenly distributed among lower and higher energies. Hence, neglect of the detector response results in a systematic bias. The sense of the bias is that observed energies below the median neutrino energy are underestimated, and those above it are overestimated. Thus, it is likely that the true energy of a neutrino event lies closer to the median energy of the distribution. While, of course, it is hopeless to determine the true energy of a single event from the observed energy, a collection of observations can be corrected for this bias.

The errors in the observed energies are reported in the above references to be Gaussian, so the response function can be written as:

$$R(E_\nu, x) = \frac{1}{\sqrt{2\pi}\Delta} e^{-(E_\nu-x)^2/2\Delta^2}, \quad (1.4)$$

where Δ is the observed error. We have fitted the reported neutrino energies and their errors to determine the empirical error functions listed in Table 1.2. In order to assess the importance of the detector response bias, we have also considered the limit of negligible errors, in which the response function becomes a delta function, and there is effectively no integral in Eq. (1.3).

At this juncture, we use the standard approximation of treating Δ as a function of x instead of E_ν . Then the integrated response function, and its first moment, become

$$\int_H^\infty R(E_\nu, x) dE_\nu \equiv A(x) = P\left(\frac{x-H}{\Delta}\right); \quad (1.5)$$

$$\int_H^\infty E_\nu R(E_\nu, x) dE_\nu \equiv xB(x) = xP\left(\frac{x-H}{\Delta}\right) + \Delta^2 R(x, H). \quad (1.6)$$

Here $P(z) = [1 + \text{erf}(z/\sqrt{2})]/2$ is the cumulative normal distribution function. In the limit of negligible errors, A and B are simply step functions: zero for $x < H$, unity for $x \geq H$.

Two general methods are used to analyze the spectrum. The so-called moment method uses only the average energy of the detected neutrinos to determine the temperature, and their number to estimate the total neutrino energy of the supernova. It is alternatively possible to use the mean square

energy (the second moment) rather than the mean energy, or even higher moments. The maximum-likelihood method, on the other hand, employs the individual energies of the events in the estimate of the temperature, and should, therefore, be more reliable. In fact, both approaches give consistent results.

The moment method requires an evaluation of the average detected neutrino energy, obtained by the taking the ratio of the zeroth and first moments of the integration of Eq. (1.3) over the observed energies E_ν . The average detected energy is thus

$$\langle E_\nu \rangle_d = \frac{\int_H^\infty x^3 f(x/T) \kappa(x) W(x) B(x) dx}{\int_H^\infty x^2 f(x/T) \kappa(x) W(x) A(x) dx} = T \frac{G_5(T)}{G_4(T)}. \quad (1.7)$$

We find it useful to refer separately to the integrals in the numerator and denominator of Eq. (1.7), which we denote by $G_5 T^6$ and $G_4 T^5$, respectively. They may be viewed as modified, truncated Fermi integrals. (The notation becomes obvious when we recall that κ is essentially proportional to x^2 .) Thus the rate of energy absorption by the detector is proportional to G_5 , while the detection rate of neutrinos is proportional to G_4 . In the limit that the efficiency W is unity, and errors are negligible, the ratio $G_5/G_4 = F_5/F_4 \simeq 5$. Note that Eq. (1.7) is an implicit function for T and it must be solved iteratively.

In the moment method, Eq. (1.7) is implicitly solved for the temperature T . In the maximum-likelihood method, one uses the entire energy distribution function $N(E_\nu)$, Eq. (1.3). In this method, one maximizes the likelihood function, or, equivalently, minimizes the quantity

$$\Lambda = -2 \sum_{i=1}^n \ln N(E_{\nu,i}), \quad (1.8)$$

where n is the number of events, with respect to the fitted parameters, in this case T . The minimum value of Λ is arbitrary, but the deviations from the minimum follow the usual χ^2 distribution, thus allowing error estimates in the usual way. Note that the maximum-likelihood method requires the normalization constant in Eq. (1.3) to be set so that the total count is independent of the fitted parameters. Thus, as in the moment method, only shape parameters of the spectrum, such as T , can be determined, but not the overall flux. We set the normalization to $\int_H^\infty N(E_\nu) dE_\nu = n$. For simultaneous fits to both detectors, the sum of the two integrals of the

two detectors is set to the total count. The fit is therefore sensitive to the relative counts in the two detectors but not to the total number of neutrinos observed.

Using either of these methods to derive the average temperature of the emitted neutrinos, the emitted antineutrino luminosity is given by

$$L_{\bar{\nu}}(t) = 4\pi R_{\bar{\nu}}^2(t) \frac{cF_3(0)}{8\pi^2(\hbar c)^3} T(t)^4, \quad (1.9)$$

where we have explicitly indicated that $L_{\bar{\nu}}, R_{\bar{\nu}}$ (the radius of the $\bar{\nu}_e$ neutrinosphere) and T are functions of time. Therefore, the counting rate in a detector is

$$\begin{aligned} \frac{dn}{dt} &= \left(\frac{R_{\bar{\nu}}(t)}{D}\right)^2 N_p \int_H^\infty x^2 f(x/T) W(x) \kappa(x) dx = \frac{\kappa_o N_p L_{\bar{\nu}}(t) G_4(t) T(t)}{4\pi D^2 F_3(0)} \\ &= M \left(\frac{50 \text{ kpc}}{D}\right)^2 \frac{L_{\bar{\nu}}(t)}{7.5 \times 10^{52} \text{ erg s}^{-1}} \frac{G_4(t) T(t)}{F_3(0)} \text{ s}^{-1}. \end{aligned} \quad (1.10)$$

Here, D is the distance to the detector and N_p is the number of protons in the detector. We have $N_p = (2/3) \times 10^{32} M$ for an H_2O detector of mass M , in kilotons. In practice, there was not enough data to find any details of the spectrum but the average temperature. If one were to assume that the temperature changed little over the time interval that the neutrinos were received, we would find for the total emitted $\bar{\nu}_e$ energy:

$$\varepsilon_{\bar{\nu}_e} = \int n dt = 7.5 \times 10^{52} \left(\frac{D}{50 \text{ kpc}}\right)^2 \frac{n}{MT} \frac{F_3(0)}{G_4} \text{ ergs}. \quad (1.11)$$

Characterizing the neutrino spectrum by a finite chemical potential does not significantly affect these results. In the cases of interest, the integrands of F_i and G_i peak near the energy $x \simeq iT$. Thus, the 1 in the Fermi factor f becomes ignorable compared to the exponential for small or moderate chemical potential μ , and we may write $f \simeq \exp[(\mu - x)/T]$. The term $e^{\mu/T}$ is thus common to all such integrals. In Eqs. (1.2), (1.7) and (1.11) these terms cancel, leaving essentially no μ dependence.

On the other hand, if one were to attempt to derive a neutrinosphere radius R from the time integral of Eq. (1.9), the unbalanced chemical potential factor in F_3 renders the result very sensitive to the assumed value of μ/T . For example, compared to the case of zero chemical potential, if

μ/T were 1 (3), the derived radius is smaller by a factor of 0.63 (0.27). It is therefore difficult to extract reliable information on the radius of the emitting surface in the case of SN 1987A.

Method of Analysis	$T_{Kamioka}$	T_{IMB}	$\varepsilon_{\bar{\nu}_e, Kamioka}$	$\varepsilon_{\bar{\nu}_e, IMB}$
With Detector Response				
Moment	2.8 ± 0.5	4.0 ± 0.7	$6.9^{+3.5}_{-3.8}$	$5.7^{+10.0}_{-2.8}$
Relative counts	$5.0^{+1.25}_{-1.0}$		$2.6^{+1.9}_{-1.6}$	
Maximum likelihood	2.8 ± 0.4	4.2 ± 1.0	$6.3^{+4.0}_{-3.1}$	$4.5^{+12.0}_{-3.4}$
Maximum likelihood (combined)	3.7 ± 0.4		$4.8^{+2.1}_{-1.8}$	
Without Detector Response				
Moment	2.8 ± 0.6	4.6 ± 0.8	$6.1^{+5.0}_{-3.0}$	$2.9^{+2.6}_{-1.6}$
Relative counts	$4.8^{+1.2}_{-1.0}$		$2.6^{+2.2}_{-1.7}$	
Maximum likelihood	2.8 ± 0.4	4.7 ± 0.8	$5.9^{+3.4}_{-2.8}$	$2.7^{+2.6}_{-1.0}$
Maximum likelihood (combined)	3.8 ± 0.4		$4.3^{+2.0}_{-1.8}$	

Table 1.3: Derived Temperatures (MeV) and $\bar{\nu}_e$ Energies (10^{52} erg)

Some results for these approaches are presented in Table 1.3. It is seen that the temperatures derived from the two detections individually differ by a factor of 1.5, although this is not statistically significant (within 1σ). What is surprising is that the two methods give nearly identical results for each experiment. We find that more complex, *e.g.*, time-dependent, spectra do not give better fits to the observed neutrino energies. The basic problem is low counting statistics, which frustrates multiparameter fits.

For comparison, in the case of negligible errors and unity efficiency, we would have $T \simeq \langle E_\nu \rangle_d / 5$. For Kamioka and IMB, this would imply temperatures of 3.3 and 6.7 MeV, respectively. The total $\bar{\nu}_e$ energy would be $\varepsilon_{\bar{\nu}_e} \simeq 19.1 \times 10^{51} n/MT$ ergs for $D = 50$ kpc, or 30.3 and 4.6×10^{51} ergs, respectively. It is clear that the combinations of efficiency and threshold are more energy dependent for IMB, in that the effective orders of the modified Fermi integrals become larger.

Note from Eqs. (1.5) and (1.6) that for a finite observed error Δ , $A(x) < B(x)$. From Eq. (1.7) we can therefore deduce that, for a given mean observed neutrino energy, including the detector response results in a decrease of the estimated temperature. It similarly follows from Eq. (1.11) that the estimated total emitted energy increases. Because the IMB ν 's lie in the tail of the Fermi distribution, beyond the peak in the spectrum, the effect of detector response is much greater for the IMB detector. Therefore, the IMB and Kamioka temperatures and, in particular, the total energies are pushed closer together.

It is possible to combine data from both detectors, assuming that they both observed the same event (*i.e.*, the total energies and temperatures were the same). This should result in improved estimates. In the moment method, this is accomplished by examining the ratio of events seen by Kamioka to those by IMB. For identical detectors this ratio is, of course, insensitive to the spectrum. Owing to the different detection efficiencies and thresholds, however, it becomes a measure of the neutrino temperature. Specifically, forcing the total energies and temperatures inferred by the two experiments to be equal gives the condition that the quantity G_4M/n must also be the same for both. Results from this calculation are included in Table 1.3.

When the maximum-likelihood method is applied to the combined data, a temperature estimate results which is intermediate between the temperatures derived for each data set separately. By contrast, the temperature deduced from the ratio of counts is in excess of those determined individually from the two detectors, although within their error estimates. This behavior underscores the higher reliability of maximum-likelihood estimates, which probe the entire probability distribution, and hence all its moments, in contrast with moment methods, which are sensitive to only a ratio of the two moments.

2. Neutron Star Binding Energy

We note that the inferred total $\bar{\nu}_e$ energy can be used to estimate the mass of the neutron star that might have formed. According to detailed models of neutrino emission, each of the six known neutrino species carries a nearly equal share of the total energy. Thus, the total binding energy of the neutron star is about 6 times $\varepsilon_{\bar{\nu}_e}$, or $1.8\text{--}4.1 \times 10^{53}$ erg. It is an empirical fact¹ (see Chapter on Neutron Star Structure) that the relatively large uncertainties in the equation of state above nuclear densities do not significantly affect the binding energy vs. gravitational mass relationship for neutron stars. A convenient fit¹ to the binding energy-mass relation is

$$E = 1.5 \times 10^{53} \left(\frac{M}{M_\odot} \right)^2 \text{ ergs}, \quad (2.1)$$

where M is the neutron star's gravitational mass. The above energy thus translates into neutron star gravitational masses in the range $1.1\text{--}1.65 M_\odot$. It is difficult to determine from the energetics alone the mass and, therefore, which explosion mechanism might have occurred in the case of SN 1987A. It is of interest, however, that this mass estimate is entirely in agreement with those derived independently from the amount of ^{56}Ni synthesized in the explosion.⁵ Furthermore, this range encompasses a large enough mass that deleptonization or thermal cooling could have triggered a collapse into a black hole *after* the bulk of the neutrinos were emitted.